

# Characterization of Immobilized Poly-L-aspartate as a Metal Chelator

ELIZABETH GUTIERREZ,<sup>†</sup>  
 THOMASIN C. MILLER,<sup>‡</sup>  
 JOSE R. GONZALEZ-REDONDO,<sup>‡</sup> AND  
 JAMES A. HOLCOMBE\*<sup>‡</sup>

Department of Chemistry and Biochemistry, University of Texas at Austin, Austin, Texas 78712, and Department of Chemistry, University of Zulia, Maracaibo, Venezuela

Poly-L-aspartic acid (PLAsp), which consists of ca. 50 Asp residues in a linear polypeptide, has been immobilized on controlled pore glass (CPG) and evaluated for its selectivity and binding strength in the complexation of metal ions from aqueous solutions. The carboxylate side chain of Asp ( $pK_a = 5.4 \pm 0.2$ ) is thought to be primarily responsible for chelation of the target metals. Of the several metals evaluated,  $\text{Eu}^{3+}$ ,  $\text{Ce}^{3+}$ ,  $\text{La}^{3+}$ ,  $\text{Cu}^{2+}$ , and  $\text{Pb}^{2+}$  exhibited good binding capacities. Quantitative determination of single-element capacities were determined for  $\text{Cu}^{2+}$  ( $12 \pm 1 \mu\text{mol/g}$  PLAsp-CPG) and  $\text{La}^{3+}$  ( $7.1 \pm 0.3 \mu\text{mol/g}$  PLAsp-CPG). Isotherms were constructed from breakthrough curves using a flow injection system. These curves were used to evaluate the effective site capacity and formation constants. A combination of moderate and strong binding sites for  $\text{Pb}^{2+}$  was detected, while moderate binding of  $\text{Cd}^{2+}$  was observed with a minimal number of strong binding sites. Several cations showed little to no binding by PLAsp-CPG (e.g.,  $\text{Na}^+$ ,  $\text{Ca}^{2+}$ ,  $\text{Mg}^{2+}$ ,  $\text{Mn}^{2+}$ ,  $\text{Co}^{2+}$ , and  $\text{Ni}^{2+}$ ). Propensity for metal binding seems to follow the trend seen for binding to carboxylates in such ligands as acetate. The polydentate binding available from the polypeptide chain significantly enhanced the binding strength with equilibrium constants in excess of  $10^9$  observed for the strong binding sites. The binding selectivity was complementary, in many cases, with the results previously reported for poly-L-cysteine immobilized on CPG.

## Introduction

Removal of heavy metals from the environment has become a major focus of waste treatment and cleanup efforts. In particular, metals such as iron, cobalt, nickel, copper, cadmium, copper, and those of the transuranium series threaten both human and environmental health through their increasing presence in industrial wastewaters.

One method proven to be particularly effective for the removal of metals from the environment is ion-exchange chromatography. Recent reviews speak to the activity involving this technique for the separation and determination of transition and rare earth elements (e.g., refs 1–3). Ion exchange has also been shown to be a relevant technology for the preconcentration and remediation of such metals (4, 5).

\* Corresponding author e-mail: holcombe@uts.cc.utexas.edu; phone: (512)471-5140; fax: (512)471-0985.

<sup>†</sup> University of Zulia.

<sup>‡</sup> University of Texas at Austin.

The ideal materials for the process of the remediation of metals through ion exchange require a certain degree of selectivity for the species of interest (i.e., metals). By using a column that only binds the target species of interest, the effective capacity of the column is enhanced due to limited competition for the binding sites by other concomitants of the sample solution. The ideal system should also provide strong selective metal binding as well as easy, on-demand release of the target metal or metals. The latter feature combined with selectivity should greatly enhance recovery and minimize post-recovery refinement of metals. Analytical preconcentration or matrix elimination could also benefit from these same characteristics.

Many biological systems seem to provide selectivity, including metal-specific binding. As an example, metallothioneins are one class of proteins that are reported to be highly selective. However, the tertiary structure of the proteins, which is believed to contribute to this selectivity, is often lost when isolated from the unique chemical environment within the cell (6). Recognizing that many metallothioneins have a large cysteine content, Autry and Holcombe (7) and Jurbergs and Holcombe (8) evaluated the utility of poly-L-cysteine (PLCys) immobilized on controlled pore glass (CPG) as a chelation material. They found that PLCys-CPG had a high degree of selectivity for the soft acid metals. For example, a formation constant of  $10^{13}$  was measured for Cd. It was postulated that the linear chain of ca. 50 cysteine residues wrapped around the target metal to provide the three-dimensional binding cavity with likely binding to the thiol groups. Uniquely, the release of the metals could be mediated by simply lowering the pH of the column eluent solution. The metals could be quantitatively released in a minimal volume of acid, thus providing optimal preconcentration factors. It was suggested that this easy release is a result of protonation of the sulfhydryl groups that displaces the metal as well as disrupts the optimal tertiary structure responsible for strong metal binding. The CPG material also remained extremely rugged despite hundreds of strips with 1 M  $\text{HNO}_3$  as well as  $\text{H}_2\text{O}_2$  oxidation, with no noticeable change in column binding capacity and strength with more than 1 year of use.

The success of the PLCys suggests the potential utility of polyamino acids or simple amino acid copolymers as selective chelators. Considering the variety of binding functionalities available from amino acids and the ease of forming the same polymer linkage (i.e., peptide bonds), the PLCys system seemed to suggest a prototype for the design of selective chelators.

Since the sulfhydryl group of Cys favors binding to soft acid metals, a contrasting, harder base functionality was sought to evaluate the altered selectivity of a different polyamino acid. The carboxylate of Asp or Glu fits this criterion. Free aspartate in a homogeneous solution can behave as a terdentate ligand with the terminal amine and carboxylate functionalities as well as the carboxylic side chain available for complexation. A number of di- and trivalent ions have been chelated and the known stability constants determined (9, 10). The chelate effect of Asp has been referenced as the source of the more favorable binding in comparison with other amino acids, including Glu (10). From this initial reasoning, poly-L-aspartic acid (PLAsp) (Figure 1) was selected for this study.

The biological importance of aspartic acid is suggested by the metal-binding behavior of proteins in organic mollusk shells. The organic matrix in mollusk shells is involved in binding calcium and ultimately in producing the calcium

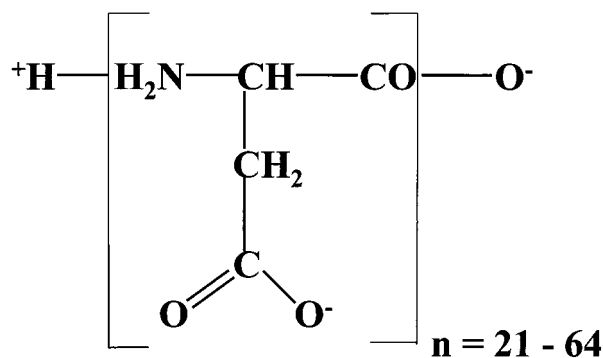


FIGURE 1. Structure of poly-L-aspartate.

carbonate crystals in the mineralization process of shell formation (11, 12). It was found that a significant portion of the protein sequence of the  $\text{Ca}^{2+}$  binding subunit is (Asp-Y) where Y is predominantly Ser and Gly (13). It is suggested that the improved conformational structure for metal binding might explain the preference for Asp in place of Glu, which contains another methyl group in the side chain.

This paper details the results for the preliminary evaluation of PLAsp immobilized on controlled pore glass (PLAsp-CPG) for metal chelation. Mindful of the contrasting character of the carboxylate ligand relative to the sulfhydryl group of PLCys, a qualitative comparison of these two immobilized polyamino acid chelators will be made.

## Experimental Section

**Instrumentation.** The flow injection manifold is shown in Figure 2 and was used to provide flow of acid, buffer, and sample to the column using an eight-roller peristaltic pump (Ismatec minicartridge MS-REGLO) and two two-way, double inlet rotary valves (Rheodyne 5020). All connections were made with 0.76 mm i.d. PTFE tubing. A 3 mm i.d.  $\times$  25 mm long glass column with 70  $\mu\text{m}$  PTFE frits (Omnifit) was packed with 0.0810 g of PLAsp-CPG. A Kel-F tee was placed between the column and the nebulizer to provide air compensation and to minimize noise. A second column packed with 0.083 g of CPG was treated by boiling the CPG in 1 M  $\text{HNO}_3$  for 30 min (i.e., the acidification step used in the preparation of the CPG for immobilization). This was used for studies of metal binding to acid activated glass.

A Perkins-Elmer model 4000 atomic absorption spectrometer with an air acetylene flame was used for determination of the metals. Hollow cathode lamps for the studied elements were operated at the currents recommended by their manufacturers. Wavelengths for Ca, Cd, Co, Cu, Fe, Mn, Na, Ni, and Pb were 422.7, 228.8, 240.7, 324.8, 248.3, 279.5, 589.0, 232.0, and 217.0 nm, respectively and were used in conjunction with a monochromator band-pass of 0.7 nm for Ca, Cd, Na, and Pb and 0.2 nm for Cu, Fe, Mn, and Ni.

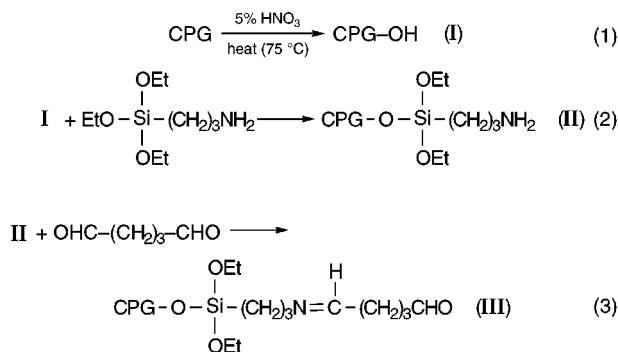
An argon inductively coupled plasma-mass spectrometer (ICP-MS) (A Varian Ultramass) was used for analysis of Al, Ce, Eu, and La on PLAsp-CPG and for the analysis of the strip solutions of the mixture of metals in both PLAsp-CPG and acid-activated glass columns.

**Reagents.** All reagents used were reagent grade unless noted. Deionized distilled water was used to prepare solutions, and all glassware was soaked overnight in 4 M  $\text{HNO}_3$  before use. Poly-L-aspartic acid (Sigma) [DP(vis) 50, MW(vis) 11,100] was used as received. Controlled pore glass (PG240-120; Sigma) had an average pore diameter of 226  $\text{\AA}$  and a mesh size of 80-120. Other reagents included 3-aminopropyltriethoxysilane (98%), glutaraldehyde (25%), DL-dithiothreitol, 5,5'-dithiobis(nitrobenzoic acid) (Sigma); hydrogen peroxide, 30% (EM Science), and disodium hydrogen phosphate. Stock solutions of  $\text{Ca}^{2+}$  (Fisher),  $\text{Cu}^{2+}$  (Baker),  $\text{Fe}^{3+}$

(Ricca), and  $\text{La}^{3+}$  (Sigma) atomic absorption standards were used to prepare the 10 ppm loading solutions for the metal-binding experiments. For  $\text{Al}^{3+}$  (Baker),  $\text{Cd}^{2+}$  (Baker),  $\text{Co}^{2+}$  (Baker),  $\text{Mn}^{2+}$  (Matheson),  $\text{Na}^+$  (Baker),  $\text{Ni}^{2+}$  (Baker), and  $\text{Pb}^{2+}$  (EM Science), the loading solutions were prepared from the reagent-grade nitrate salt.

**Procedures.** *Determination of  $pK_a$  of PLAsp.* The  $pK_a$  of PLAsp was determined by dissolving 0.016 g of the sodium salt in ca. 50 mL of water. The solution was acidified with HCl to pH < 4 and potentiometrically titrated with  $2.5 \times 10^{-3}$  M NaOH. Curve fitting was used with the titration curve data to verify the  $pK_a$  of the acid.

*Preparation of Acid-Activated CPG, Silanized CPG, and Glutaraldehyde CPG.* The immobilization procedure has been described previously (8) and represents a modification of the approach originally proposed by Masoom and Townsend (14). Equations 1-3 show the steps leading to the immobilization of a target chelator on CPG through the formation of an imine at the glutaraldehyde terminus of III.



The CPG was activated by boiling the glass in 5%  $\text{HNO}_3$  for 150 min. The CPG was then silanized using 3-aminopropyltriethoxysilane to provide the amino terminus for final linking with glutaraldehyde before eventual attachment of the target chelating amino acid or protein.

*Immobilization of PLAsp-CPG.* A total of 50 mg of PLAsp dissolved in 20 mL of pH 4-5 phosphate buffer with ca. 1 g of glutaraldehyde-CPG was used in the immobilization step. Once immobilization was complete, the PLAsp-CPG was sieved through 200 mesh screens to remove unbound PLAsp. Approximately 0.1 g of PLAsp-CPG was needed to fill the microcolumn.

*Binding of Metals to PLAsp-CPG.* The flow injection system shown in Figure 2 was employed in all experiments after a 15-min warmup of pumps and tubing. Before binding experiments were performed, 0.1 M  $\text{HNO}_3$  was passed through the column for 30 s at 1 mL/min followed by 0.05 M ammonium acetate buffer (pH = 7.0) for the same period of time and at the same flow rate. After initial conditioning, complete breakthrough curves were obtained for several metals ( $\text{Ca}^{2+}$ ,  $\text{Cd}^{2+}$ ,  $\text{Co}^{2+}$ ,  $\text{Cu}^{2+}$ ,  $\text{Fe}^{3+}$ ,  $\text{Mn}^{2+}$ ,  $\text{Na}^+$ ,  $\text{Ni}^{2+}$ , and  $\text{Pb}^{2+}$ ) by monitoring the flame atomic absorption signal as a 10 ppm solution of the target metal was passed through the microcolumn. Similarly, breakthrough curves for  $\text{La}^{3+}$  and  $\text{Al}^{3+}$  were obtained by monitoring the time-dependent signal for the ICP-MS because of the increased sensitivity over a  $\text{C}_2\text{H}_2$ /air flame AA system. After ca. 20 min (or when a nearly constant, high absorbance suggested that the effluent concentration had reached the influent concentration), the sample flow was stopped. Buffer was then passed through the lines for 15 s to remove metal-containing solution from the column dead volume and line tubing. The 0.1 M  $\text{HNO}_3$  was switched in-line to strip the metals into a 25-mL volumetric flask for subsequent analysis. While past studies have shown that only a few hundred microliters was needed to strip many metals from the column, 25 mL was employed

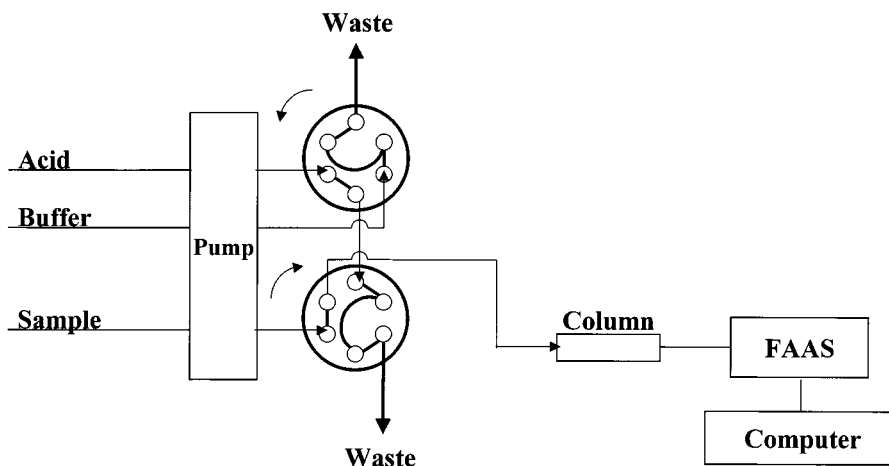


FIGURE 2. Flow injection analysis system used to provide flow of acid, buffer, and sample to the column using an eight-roller peristaltic pump with two-way double inlet valves. The configuration shown here illustrates the valves positioned such that only sample is delivered to the column.

to ensure complete removal and to have sufficient sample to conduct the needed analyses. Acidified standards, which were not retained by the column, were pumped through the system after stripping. The signals from these standards were used to construct a calibration curve.

**Binding of Lanthanides to PLAsp-CPG.** A single solution at pH 7 containing 10 ppm of  $Ce^{3+}$ ,  $Eu^{3+}$ , and  $La^{3+}$  was passed through the PLAsp-CPG column without FAA monitoring of effluent. After 20 min of solution flow at a rate of 1 mL/min, acid was passed through the column to strip the metals into a 25-mL volumetric flask. These solutions were then analyzed by ICP-MS to determine the relative binding capacities of these metals. The procedure was then repeated for single 10 ppm metal solutions of each of these lanthanides.

**Metals Binding Studies on PLAsp-CPG and Modified Surface of CPG.** A single solution at pH 7.0 containing 10 ppm of  $Al^{3+}$ ,  $Cu^{2+}$ ,  $La^{3+}$ ,  $Pb^{2+}$ ,  $Ni^{2+}$ , and  $Cd^{2+}$  was passed through the PLAsp-CPG column without FAA monitoring of effluent.  $Fe^{3+}$  was not used since it appeared that the presence of the other metals initiated the precipitation of  $Fe(OH)_3(s)$  at pH = 7.0. The loading, stripping, and analysis procedure described above for the lanthanides was used for this multimetal solution on the PLAsp-CPG and was also repeated for the acid-activated CPG column.

The uptake of  $Cd^{2+}$ ,  $Cu^{2+}$ ,  $Ni^{2+}$ , and  $Pb^{2+}$  was evaluated separately on each of the three modified CPG columns: 0.083 g of acid-activated CPG, 0.077 g of silanized CPG, and 0.078 g of glutaraldehyde CPG, respectively, at pH 7.0 with metal influent concentrations of 10 ppm and influent flow rates of 1.0 mL/min. The loading and stripping procedure was the same as that described for the binding analysis of singular metals to the PLAsp-CPG column.

## Results and Discussion

Complexation by PLAsp should be enhanced by deprotonation of the carboxylate side chains, that is, the solution pH should be greater than the  $pK_a$  of PLAsp. The  $pK_a$  reported for the carboxylate side chain for a homogeneous solution of aspartic acid is between 3.0 and 4.7 at 25 °C (15). According to Sela and Katchalski (16), it might be expected that the  $pK_a$  values of copolymers of amino acids with polar side chains would be influenced by electric charge effects, size and shape of the peptide, and dissociation of specific groups in the chain. Specifically, their arguments would suggest that the  $pK_a$  should increase with an increasing number of aspartic acid groups in the PLAsp polymer. This is consistent with the results from the titration of PLAsp where the  $pK_a$  was

determined to be  $5.4 \pm 0.2$ . The binding experiments conducted in this study were run at pH = 7.0, where the extent of deprotonation of the side chains would be greater than 95%.

Breakthrough curves were analyzed by looking at the concentration of the analyte in the effluent phase ( $C_m$ ) as a function of the influent volume ( $V$ ) passed through the column. Alternatively, the breakthrough curve can be converted to an adsorption isotherm by

$$C_s = \frac{(C_m^0 V - \int_0^V C_m dV)}{m} \quad (4)$$

where  $C_s$  is the metal bound to the stationary phase (mol/g) after a volume  $V$  is passed through the column,  $C_m^0$  is the molar influent concentration,  $C_m$  is the mass of PLAsp-CPG used in the column. A plot of  $C_s$  versus  $C_m$  yields the binding or adsorption isotherm for the flow system. It has been shown for PLCys-CPG, which used the same column and support geometry as this study, that mass transport limited the attainment of equilibrium in the column. However, at a low rate of 0.5 mL/min, the bound-to-free ratio in the column was ca. 80% of the value expected for complete attainment of equilibrium (8). Hence, analysis of the flow data from the FIA system at ca. 1.0 mL/min provides only an indication of the equilibrium values and a picture of the effective capacity and effective  $K_f$  but does not yield the thermodynamic values for metal binding to the polyamino acid ligands. Similarly, the capacity of the column should represent the total number of binding sites. However, when weak binding sites are present, the maximum amount bound to these sites is concentration dependent since not all of these sites are expected to be filled even when  $C_m = C_m^0$  during the breakthrough experiment.

After converting the breakthrough data to isotherms, curve fitting was used to fit the data to the general expression for a multisite equilibria system (17):

$$C_s = C_m \sum_{i=1}^n \frac{K_i L_i^0}{1 + K_i C_m} \quad (5)$$

where  $K_i$  and  $L_i^0$  are the formation constant and total number of binding sites for the  $i$ th site. Figure 3 shows the data and fit for  $Cu^{2+}$  using a maximum of three distinct binding sites. Table 1 shows the features resulting from this

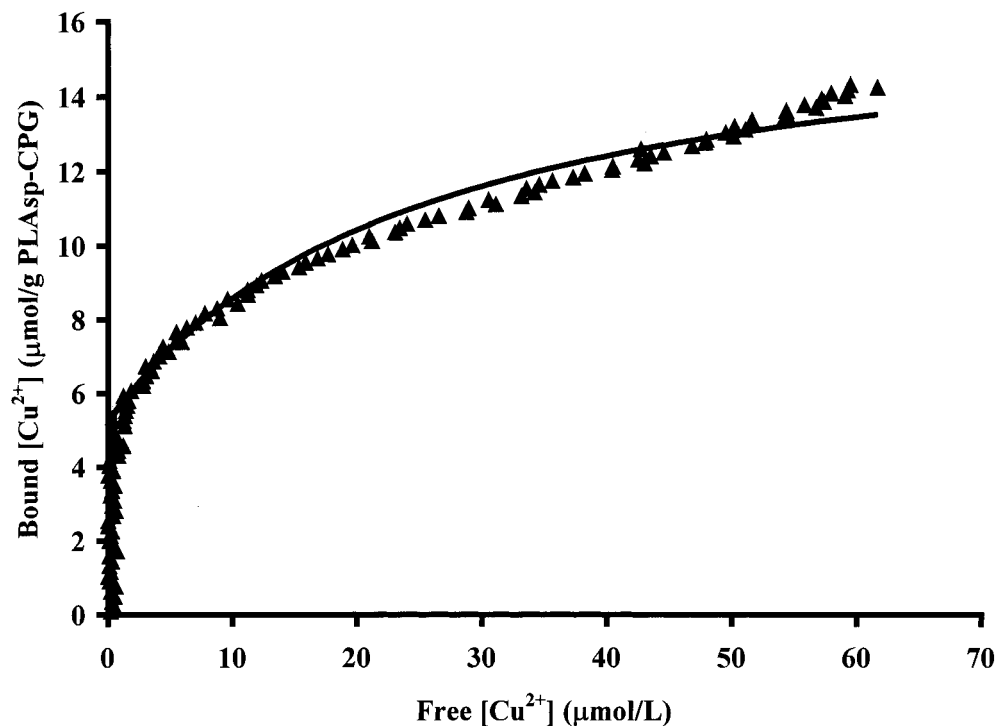


FIGURE 3. Example of experimental data and fit using eq 2 for the isotherm of  $\text{Cu}^{2+}$  binding on PLAsp-CPG using a maximum of three distinct binding sites. The data represent effective formation constants and the number of sites reported in Table 1.

TABLE 1. Effective Stability Constants and Number of Binding Sites for Cu-PLAsp Complexes<sup>a</sup>

effective conditional stability constant ( $K_{\text{eff}}$ )	no. of binding sites, $L^{\circ}$ ( $\mu\text{mol/g}$ )
$K = 6.43 \times 10^{14}$	5.25
$K = 4.04 \times 10^4$	11.6
$K = 1.71 \times 10^1$ <sup>b</sup>	0.0294

<sup>a</sup> pH = 7.0, flow rate = 1.0 mL/min. <sup>b</sup> Assignment of weak sites is inherently difficult due to incomplete coverage of sites.

TABLE 2. Breakthrough Capacity and Strip Recovery of Metals on the PLAsp-CPG Column<sup>a</sup>

metal ion	capacities ( $\mu\text{mol/g}$ ) determined from breakthrough curve	capacities ( $\mu\text{mol/g}$ ) determined from acid strip	recovery (%)
$\text{Fe}^{3+}$	$36 \pm 1$	$20 \pm 4$	54
$\text{Al}^{3+}$	$26 \pm 1$	$12 \pm 10$	46
$\text{Cu}^{2+}$	$12 \pm 1$	$12 \pm 1$	100
$\text{La}^{3+}$	$7.1 \pm 0.3$	$6.3 \pm 0.4$	89
$\text{Pb}^{2+}$	$4.6 \pm 0.1$	$4.5 \pm 0.1$	98
$\text{Cd}^{2+}$	$3.7 \pm 0.5$	$3.1 \pm 0.1$	84
$\text{Ni}^{2+}$	$3.1 \pm 0.2$	$2.9 \pm 0.1$	94
$\text{Co}^{2+}$	$1.6 \pm 0.1$	$1.6 \pm 0.1$	100
$\text{Mn}^{2+}$	$1.5 \pm 0.2$	$1.4 \pm 0.1$	93
$\text{Ca}^{2+}$	$1.0 \pm 0.1$	$1.2 \pm 0.1$	120
$\text{Na}^{+}$	<0.1	<0.1	

<sup>a</sup> pH = 7.0, flow rate = 1 mL/min, triplicate measurements.

curve fit. Again, the data represents effective formation constants and number of sites. The number of strong and moderate sites have now been extracted from the less descriptive "total capacity" of Table 2, which was garnered from the simple analysis of the breakthrough data using eq 4.

It is not possible to obtain unambiguous values for  $K_i$  and  $L_i^{\circ}$  for the weaker sites from breakthrough data using a single influent concentration. However, their product,  $K_i \cdot L_i^{\circ}$ ,

provides an estimate of bound:free ratio when  $L_i^{\circ}$  is large. Further studies to delineate the values using different influent concentrations were not conducted since these weak binding sites are considered to be of only marginal utility in the intended use of the column.

The effective capacity of the PLAsp-CPG column (expressed as total  $\mu\text{mol}$  of metal bound/g of PLAsp-CPG) was determined by eq 4 using the breakthrough curve data. These values were compared with the amount of analyte metal found in the strip solution and were used to determine the percent recovery of metal from the column. As stated earlier, the ideal metal-binding system should allow for strong selective metal binding to the column as well as on-demand release of the metal. The data in Table 2 also show that quantitative recoveries for most of the metals are achieved using 0.1 M  $\text{HNO}_3$  eluent. This is most likely due to a  $\text{H}^{+}$  displacement combined with a conformational change disrupting the optimal tertiary structure responsible for strong binding upon the lowering of pH (18).

It is suggested from the large breakthrough capacities for  $\text{Al}^{3+}$  and  $\text{Fe}^{3+}$  reported in Table 2 that these ions bind very strongly to PLAsp-CPG. This is in agreement with the prediction made by Gulumian et al. (19) for the binding of  $\text{Al}^{3+}$  and  $\text{Fe}^{3+}$  to carboxylate ligands. However, these metals exhibit only limited recoveries when stripped from the column with acid. This behavior may be caused by the precipitation of the metal hydroxides onto the column during loading.

Thermodynamics predict that at a concentration of 10 ppm and pH 7.0,  $\text{Fe}^{3+}$  will precipitate as  $\text{Fe}(\text{OH})_3$ , and  $\text{Al}^{3+}$  will precipitate as  $\text{Al}(\text{OH})_3$ . If the precipitate existed, it is possible that some elution of the particles during loading may account for the lower than expected mass during the strip. Interestingly, the solutions that were prepared for breakthrough analysis remained clear and did not demonstrate any turbidity throughout the duration of the experiment. However, some impurity or condition of the column could have initiated precipitation of the metal hydroxide as the solutions entered the column and equilibrated.

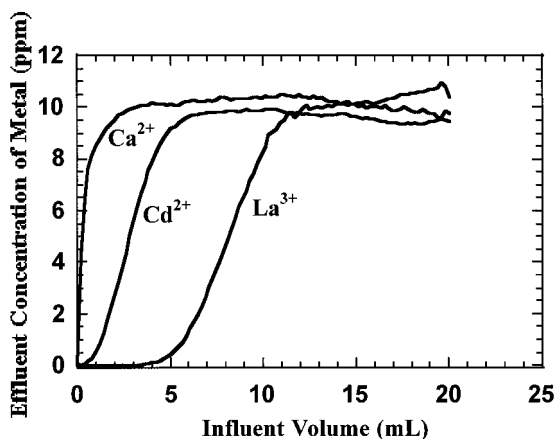


FIGURE 4. Breakthrough curves of  $\text{Ca}^{2+}$ ,  $\text{Cd}^{2+}$ , and  $\text{La}^{3+}$  on PLAsp-CPG as example of metals exhibiting minimal binding, moderately strong binding, and strong binding, respectively.

Since no precipitation was directly observed in solution or on the column, no confirmed explanation can be given for the behavior of  $\text{Al}^{3+}$  and  $\text{Fe}^{3+}$ . Therefore, the analyses and results of these two ions are included with the data reported without any definitive statement about the binding of  $\text{Al}^{3+}$  and  $\text{Fe}^{3+}$  to PLAsp-CPG.

The breakthrough curves for  $\text{La}^{3+}$ ,  $\text{Cd}^{2+}$ , and  $\text{Ca}^{2+}$  are shown in Figure 4. These represent the extremes of binding to PLAsp-CPG, with  $\text{La}^{3+}$  showing the presence of strong binding sites ( $K_{\text{eff}} > 10^8$ ) as indicated by the extended baseline region between 0 and 4.5 mL;  $\text{Cd}^{2+}$  showing moderately strong binding sites ( $10^8 > K_{\text{eff}} > 10^4$ ); and  $\text{Ca}^{2+}$  exhibiting minimal binding. For those metals for which complete breakthrough curves were obtained,  $\text{Cu}^{2+}$ ,  $\text{Pb}^{2+}$  and  $\text{La}^{3+}$  displayed measurable strong site capacities while  $\text{Cd}^{2+}$  and  $\text{Ni}^{2+}$  exhibited no measurable strong sites. The remaining metals displayed very little binding to the PLAsp column. Table 2 summarizes the results for this set of metals. In brief, the capacities determined from the breakthrough curve were in the order  $\text{Cu}^{2+} > \text{La}^{3+} > \text{Pb}^{2+} > \text{Cd}^{2+} > \text{Ni}^{2+} > \text{Co}^{2+} > \text{Mn}^{2+} > \text{Ca}^{2+} > \text{Na}^+$ . This trend is in basic agreement with that reported by Gulumian et al. (19) for negative oxygen donors, such as carboxylates, in biological systems. This type of oxygen donor is characterized as a very hard donor group preferring to complex with metals classified as the hard metal ions such as  $\text{Cu}^{2+}$  and  $\text{La}^{3+}$  (20). However, in the trend given above, it is clearly shown that the PLAsp carboxylate side chains also have a tendency to bind some of the softer metal ions such as  $\text{Cd}^{2+}$  and  $\text{Pb}^{2+}$ . According to Stumm and Morgan (21), hard acid metal ions have an absolute preference in aqueous solution for hard donor ligands containing oxygen such as a carboxylate. Softer metal acids prefer soft donor ligands such as sulfhydryl groups. However, soft metal acids also are able to form strong complexes in aqueous solution with ligands of the type  $-\text{CO}-\text{N}-\text{R}$ , which is present in the peptide bond. Since the PLAsp contains ca. 50 peptide bonds per chain, it is reasonable that the softer acid metals may also be binding to these sites.

The PLAsp carboxylate side chains do not seem to have any affinity for a specific metal electron configuration or spatial geometry of ligand coordination. The wide range of metal-binding modes that can be adopted reflects versatility afforded by the carboxylate ligand side chains when attached to a flexible polymer backbone. Rardin et al. (22) have shown that up to three metal ions can bind to a single carboxylate ligand with structurally distinct coordination to one or more of the four available electron lone pairs on the two oxygen atoms of the carboxylate anion. Coordination versatility may also be explained by the flexibility offered by a chain of 50

TABLE 3. Binding Capacity of Select Lanthanides to PLAsp-CPG in Noncompetitive (Single Metal, 10 ppm Influent Solution) and Competitive (Multimetal Influent Solution Containing 10 ppm of Each Metal) Binding Solutions<sup>a</sup>

metal ion	capacities ( $\mu\text{mol/g}$ ) from	
	single	multimetal solution
$\text{Ce}^{3+}$	$7.4 \pm 0.2$	$1.8 \pm 0.1$
$\text{Eu}^{3+}$	$7.4 \pm 0.1$	$4.7 \pm 0.1$
$\text{La}^{3+}$	$7.1 \pm 0.3$	$0.62 \pm 0.02$

<sup>a</sup> pH = 7.0, flow rate = 1.0 mL/min, triplicate measurements.

carboxylate residues which allows for more relaxed spatial ligand geometries around a single metal cation.

**Comparison of Binding Characteristics of PLAsp with PLCys.** As stated above, the carboxylic acid side chains in PLAsp act as hard donor ligands, preferentially binding with hard and moderately hard acid metals. The thiol side chains of PLCys, on the other hand, act as soft donor ligands, preferentially binding to soft and moderately soft metal acids. For example, PLAsp binds the hard metal acids of  $\text{Cu}^{2+}$  and  $\text{La}^{3+}$ , and PLCys has a large strong site capacity for  $\text{Cd}^{2+}$  and  $\text{Pb}^{2+}$  (8).

One specific example showing the difference between the binding characteristics of PLAsp and PLCys is their behavior toward  $\text{Cu}^{2+}$ . Both PLAsp and PLCys showed significant binding when  $\text{Cu}^{2+}$  was used as the influent. However, it has been shown that  $\text{Cu}^{2+}$  oxidizes PLCys (18, 23), and it has been demonstrated that copper is likely bound to the PLCys-CPG system as  $\text{Cu}^+$ , a soft metal acid. In contrast, PLAsp is not readily oxidized and is unlikely to be oxidized by  $\text{Cu}^{2+}$ . Thus, it is likely that PLAsp binds  $\text{Cu}^{2+}$ .

**Analysis of the Lanthanides.** Environmental interest in remediation continues for the rare earth elements (REE) and, in particular, the transuranium (TRU) elements.  $\text{La}^{3+}$ ,  $\text{Ce}^{3+}$ , and  $\text{Eu}^{3+}$  were selected as surrogate test elements for evaluation of the binding characteristics of PLAsp for REEs and TRUs. The relative binding capacities of each individual lanthanide and the competitive binding capacities of each metal in the mixed lanthanide analysis on PLAsp-CPG are listed in Table 3. The PLAsp-CPG system showed a similar, very high affinity for the three individual lanthanide elements with preferential binding in the order of  $\text{Eu}^{3+} > \text{Ce}^{3+} > \text{La}^{3+}$  in the mixed lanthanide analysis. This is in agreement with the conclusions of Snyder et al. (24), who observed that, for the trivalent lanthanides, binding increases with decreasing effective ionic radius. However, the binding differences between the lanthanide metals are expected to be very small since they all have the same charge and similar ionic radius. It is also interesting to note that the average amount of individual lanthanide bound to PLAsp-CPG is  $\sim 7.2 \mu\text{mol/g}$ , which is very similar to the total amount of lanthanides bound from the mixed lanthanide solution. This indicates that PLAsp-CPG may contain a finite number of sites capable of binding to metals with the approximate ionic radii of the lanthanides. These preliminary results indicate that PLAsp-CPG may be a very good chelation agent for binding other REEs and TRUs.

**Mixed Metal Affinity Study on PLAsp-CPG.** A multi-metal solution containing 10 ppm each of the different metals that individually bound strongly to the PLAsp-CPG column (except  $\text{Fe}^{3+}$ ) was prepared and passed through the column to obtain a general sense of how the column would behave when exposed to many metals at once. The results for this mixed metal solution are given in Table 4. The binding capacity trend shown for these metals is again consistent with that described for the breakthrough studies for a strong carboxylate donor ligand. The capacities for the competitive

**TABLE 4. Strip Capacity Determined from Analysis of Acid Stripped Solutions after Loading a Column with a Solution Containing Each of the Test Metals at 10 ppm<sup>a</sup>**

metal ion	strip capacity on PLAsp-CPG ( $\mu\text{mol/g}$ )	strip capacity on activated CPG ( $\mu\text{mol/g}$ )
Al <sup>3+</sup>	33 $\pm$ 6	29 $\pm$ 4
Cd <sup>2+</sup>	0.71 $\pm$ 0.04	0.41 $\pm$ 0.07
Cu <sup>2+</sup>	14 $\pm$ 2	7.3 $\pm$ 0.3
La <sup>3+</sup>	7.4 $\pm$ 1.3	2.7 $\pm$ 0.3
Ni <sup>2+</sup>	0.91 $\pm$ 0.10	0.54 $\pm$ 0.17
Pb <sup>2+</sup>	4.5 $\pm$ 0.5	4.5 $\pm$ 0.1

<sup>a</sup> PLAsp-CPG and activated CPG columns were used (pH = 7.0, flow rate = 1 mL/min, triplicate measurements).

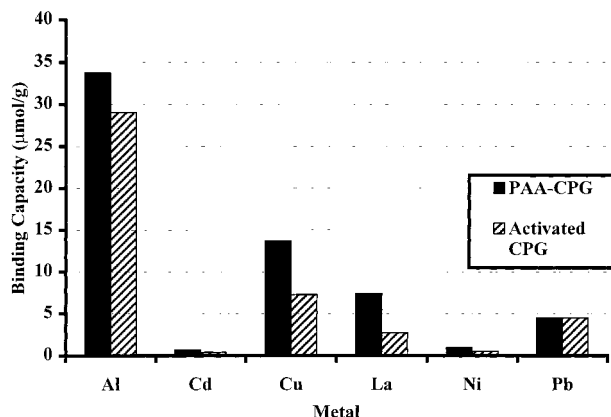


**FIGURE 5. Comparison of metal-binding affinities (in  $\mu\text{mol}$  of metal/g of column) for various metals on PLAsp-CPG and activated CPG. Mass of PLAsp-CPG column is 0.081 g, and mass of activated CPG column is 0.083 g.**

binding experiment were in the order Al<sup>3+</sup> > Cu<sup>2+</sup> > La<sup>3+</sup> > Pb<sup>2+</sup> > Ni<sup>2+</sup> > Cd<sup>2+</sup>.

The capacities for the metals on the PLAsp-CPG system for the mixed metal solution are similar to those reported in the breakthrough section for the strong binding metals (Cu<sup>2+</sup>, La<sup>3+</sup>, Pb<sup>2+</sup>). For example, the capacity determined for the single-element Cu<sup>2+</sup> solution on PLAsp-CPG was 12  $\pm$  1  $\mu\text{mol/g}$  PLAsp-CPG. In the mixed metal study, the capacity for Cu<sup>2+</sup> was 14  $\pm$  2  $\mu\text{mol/g}$  PLAsp-CPG. The capacities for Ni<sup>2+</sup> and Cd<sup>2+</sup> determined from the mixed metal-binding solution are significantly smaller than for their individual metal-binding solutions. This is most likely due to the fact that the PLAsp-CPG binding sites are preferentially filled by the stronger binding metals in a mixed metal solution leaving minimal remaining sites for the binding of weaker metal acids.

**Binding of Metals to Acid-Activated CPG, Silanized CPG, and Gluteraldehyde CPG.** Since complete coverage of the sites on the CPG by PLAsp may not occur during the immobilization procedure, the uptake of different metals by the acid-treated glass was considered. While it is difficult to quantitatively determine the affinity and number of silanol binding sites on the CPG after PLAsp has been bound to the glass, the binding of the acidified CPG only gives an indication of whether the siloxyl groups on the CPG are a potential source of binding. Table 4 provides the results of the same metal mixture described above for CPG without immobilized PLAsp. Figure 5 shows the amount of metal bound to both the PLAsp-CPG and the activated CPG system. It is expected that, since both the acid-activated glass and the PLAsp carboxylate groups are both oxygen-based ligands, their metal-binding properties should be very similar. Indeed, we observe that both columns significantly bind Cu<sup>2+</sup>, Al<sup>3+</sup>, and Pb<sup>2+</sup> with a similar binding trend for all metals. At first glance,

**TABLE 5. Binding Capacity of the CPG System during Different Stages of PLAsp Immobilization<sup>a</sup>**

metal ion	capacity ( $\mu\text{mol/g}$ )			
	acid-activated CPG	silanized CPG	gluteraldehyde CPG	PLAsp-CPG
Cd <sup>2+</sup>	0.41	<0.1	<0.1	3.1
Cu <sup>2+</sup>	7.6	1.9	4.1	12
Ni <sup>2+</sup>	0.54	<0.1	<0.1	3.1
Pb <sup>2+</sup>	11	4.1	2.7	4.6

<sup>a</sup> pH = 7.0, flow rate = 1.0 mL/min.

it may seem that the carboxylate groups of the immobilized PLAsp contribute very little to the metal-binding characteristics of the PLAsp-CPG as compared to the silanol groups of the CPG. However, while the capacities are significant for Cu<sup>2+</sup>, Al<sup>3+</sup>, and Pb<sup>2+</sup> on the acid-activated as compared to the values for the metal bound to the PLAsp-CPG system, none of the values are higher than the amount of metal bound to the PLAsp-CPG. Additionally, it must be noted that the aminopropyl linker or PLAsp may significantly or even completely cover the sites responsible for binding metal to acidified CPG during the immobilization procedure. In light of these arguments, it is likely that metal binding to the CPG silanol groups is not a main component of the metal-binding characteristics of the PLAsp system.

To test this hypothesis, the affinity of the glass for target metals of interest (Cd<sup>2+</sup>, Cu<sup>2+</sup>, Ni<sup>2+</sup>, and Pb<sup>2+</sup>) was tested on three different columns representing the different stages of the immobilization procedure (acid activation, silanization, and gluteraldehyde linkage) to anchor the polyamino acid chelator on the glass support. Table 5 shows the breakthrough capacities for the different metals on the three different columns. The main trend that is illustrated by the data is that the capacity of the glass for all metals decreases significantly when the terminal group on the glass is changed from an acid-activated silanol group to a silanized aminopropyl group. The capacity for Cu<sup>2+</sup> then increases as the gluteraldehyde linkage is attached to the glass as expected. The capacity then increases for all metals with the PLAsp attached. From these trends, it can be assumed that the metal binding to the PLAsp-CPG column is mainly due to the polyamino acid substrate with minimal contributions from unblocked silanol and gluteraldehyde groups. Therefore, there should be no difficulty in assigning metal binding to the polyamino acid chelator.

**Potential Selectivity for Metals in Environmental Samples.** The results from the current study show that PLAsp has complementary chelating behavior to PLCys demonstrating strong binding to Ce<sup>3+</sup>, Cu<sup>2+</sup>, Eu<sup>3+</sup>, La<sup>3+</sup>, and Pb<sup>2+</sup> and has significantly less affinity for soft acid metals such as Cd<sup>2+</sup> and Ni<sup>2+</sup>. Capacities for the high affinity metals are in the order of tens of micromoles per gram of PLAsp-CPG and are similar to that observed between PLCys-CPG and Cd<sup>2+</sup>. The binding selectivity for PLAsp is not simply an affinity for the hard acid metals since it exhibits little propensity toward Ca<sup>2+</sup> and Na<sup>+</sup>. Its selectivity is further punctuated by its minimal binding to Co<sup>2+</sup>, Ni<sup>2+</sup>, and Mn<sup>2+</sup>.

The possibility of using this material for remediation of the rare earth elements and, in particular, the transuranium elements is suggested by the favorable binding of Eu<sup>3+</sup>, Ce<sup>3+</sup>, and La<sup>3+</sup>. The selectivity toward Cu<sup>2+</sup> suggests interesting applications in solution cleanup or polishing where the toxicity of copper on plants and microorganisms might be of concern (e.g., ref 25).

Preconcentration or matrix isolation of trace and ultratrace metals from samples containing high concentrations of the alkali and alkaline earth salts as a matrix is not uncommon. PLAsp, like PLCys, seems to show little affinity for these group

I and II ions. Thus, the possibility of selective exclusion of these matrix components and minimization of competition for binding sites on the PLAsp appears to be likely.

### Acknowledgments

This work was supported by a grant from the Gulf Coast Hazardous Substance Research Center. We would like to thank Maury E. Howard for her contributions to the CPG analysis. E.G. would like to express her appreciation for the support of the University of Zulia, Maracaibo, Venezuela.

### Literature Cited

- (1) Robards, K.; Clarke, S.; Patsalides, E. *Analyst* **1988**, *113*, 1757–1779.
- (2) Robards, K.; Starr, P.; Patsalides, E. *Analyst* **1991**, *116*, 1247–1273.
- (3) Kumar, M. *Analyst* **1994**, *119*, 2013–2024.
- (4) Reed, B. E.; Lin, W.; Matsumoto, M. R.; Jensen, J. N. *Water Environ. Res.* **1997**, *69*, 444–462.
- (5) Reed, B. E.; Matsumoto, M. R.; Jensen, J. N.; Viadero, Jr., R. V.; Lin, W. *Water Environ. Res.* **1998**, *70*, 449–473.
- (6) Anderson, B. Ph.D. Thesis, University of Texas at Austin, 1994.
- (7) Autry, H. A.; Holcombe, J. A. *Analyst* **1995**, *120*, 2643–2647.
- (8) Jurbergs, H. A.; Holcombe, J. A. *Anal. Chem.* **1997**, *69*, 1893–1898.
- (9) Gharib, F.; Zare, K. *J. Chem. Eng. Data* **1995**, *40*, 1214–1216.
- (10) Bottari, E.; Festa, M. R.; Jasionowski, R. J. *Coord. Chem.* **1989**, *20*, 209–217.
- (11) Halloran, B. A.; Donachy, J. E. *Comp. Biochem. Physiol.* **1995**, *111B*, 221–231.
- (12) Wheeler, A. P.; George, J. W.; Evans, C. A. *Science* **1981**, *212*, 1397–1398.
- (13) Weiner, S.; Hood, L. *Science* **1975**, *212*, 987–989.
- (14) Masoom, M.; Townshend, A. *Anal. Chim. Acta* **1984**, *166*, 111–118.
- (15) Dawson, R. M. C.; Elliot, D. C.; Elliot, W. H.; Jones, K. M. *Data for Biochemical Research*, 3rd ed.; Oxford Sciences Publications: Oxford, 1986.
- (16) Sela, M.; Katchalski, E. *J. Am. Chem. Soc.* **1956**, *79*, 3986–3989.
- (17) Giesy, J. P.; Alberts, J. J. *Hydrobiologia* **1989**, *189*, 659–679.
- (18) Howard, M. E.; Jurbergs, H. A.; Holcombe, J. A. *J. Anal. At. Spectrom.* Submitted for publication.
- (19) Gulumian, M.; Hancock, R. D.; Rollin, H. B. In *Handbook of Metal–Ligand Interactions in Biological Fluids*; Burton, G., Ed.; Marcel Dekker: New York, 1995; Vol. 1, p 108.
- (20) Glusker, J. P. *Adv. Protein Chem.* **1991**, *42*, 1–76.
- (21) Stumm, W.; Morgan, J. J. *Aquatic Chemistry, Chemical Equilibria and Rates in Natural Waters*, 3rd ed.; John Wiley & Sons: New York, 1996.
- (22) Rardin, R. L. *New J. Chem.* **1991**, *15*, 417–430.
- (23) Howard, M.; Jurbergs, H.; Holcombe, J. A. *Anal. Chem.* **1998**, *70*, 1604–1609.
- (24) Snyder, E.; Buoscio, B.; Falke, J. *Biochemistry* **1990**, *29*, 3937–3943.
- (25) Kozlowski, H.; Pusino, A.; Swiatek, J.; Spsychala, J.; Glowiak, T.; Micera, G.; Gessa, C. *J. Agric. Food Chem.* **1997**, *38*, 1989–1992.

Received for review November 13, 1998. Revised manuscript received February 22, 1999. Accepted March 1, 1999.

ES981166R